2014 Canada-China Conference on Advanced Reactor Development (CCCARD-2014)
Niagara Falls Marriott Fallsview Hotel & Spa, Niagara Falls, Ontario, Canada, April 27-30, 2014.

CCCARD2014-045

PRELIMINARY NUMERICAL MODELING OF NO-CORE-MELT IN THE GENERATION IV CANADIAN SCWR

Graeme Schmidt[1], Metin Yetisir[2], John A. Goldak[1]
[1] Carleton University, Ottawa, Ontario, Canada
[2] Atomic Energy of Canada Limited, Chalk River, Ontario, Canada

Abstract

The thermal flux through a reference design Generation IV Canadian SCWR (Supercritical Water Reactor) fuel channel was computed using FEM software (VrSuite). Preliminary calculations determined these fluxes to be q = 2,792[W/m] (inlet) and q = 4,287[W/m] (outlet) for normal operation, and q = 5,496[W/m] for accident conditions. These results would suggest that, as an outcome of thermal expansion and contracting gaps between fuel channel components, it is possible to minimize heat loss to the heavy water moderator in normal operation while allowing higher heat transfer rates at LOCA (Loss of Coolant Accident) conditions needed to cool the fuel - a concept termed "no-core-melt" by AECL (Atomic Energy of Canada Limited). Using this reference design as a benchmark, other geometries should be simulated in order to ascertain the optimum configuration for achieving no-core-melt.

Introduction

Canada is developing a next generation (Generation IV) reactor concept that uses supercritical water as coolant. This reactor concept is commonly known as the Canadian Supercritical Water-Cooled Reactor (Canadian SCWR). Following Canada's past experience with pressure tube heavy-water reactors, i.e. the CANDU®[3] reactor, the Canadian SCWR concept also uses pressure tubes. Pressure tubes are surrounded by, and in direct contact with, the low-pressure, low-temperature heavy water moderator. In order to limit the heat loss to the moderator at normal conditions and to prevent the pressure tube from being exposed to supercritical flow conditions, a ceramic insulator is placed between the pressure tube and the fuel bundle.

At accident conditions, the reactor is shutdown within seconds but the unstable transmuted elements in the fuel continue to fission in an exponentially decaying fashion. The heat released by these reactions is called the "decay heat". If not removed by a cooling mechanism, decay heat would cause the fuel temperatures to increase and, ultimately, result in the melting of the fuel. A safety limit is then placed on both channel power and peak pin rating to avoid fuel melting.

The ceramic insulator, liner tubes encasing it, and the manufacturing tolerances are selected such that the heat loss from the fuel channels to the moderator is minimized at normal operating conditions while allowing decay heat to escape during accident conditions to avoid fuel melting. This is possible in the Canadian SCWR concept because of the unique features of the pressure

[3] CANDU – Canada Deuterium Uranium, a registered trademark of Atomic Energy of Canada Limited (AECL).

tube core that allows decay heat removal by passive radiative cooling of the fuel bundle to the insulator and conductive heat transfer out to the pressure tube, and subsequently to the moderator. Hence, as long as the pressure tubes and moderator are intact, the fuel and fuel cladding will not reach melting temperatures. In the Canadian SCWR, this is called the "no-core-melt concept".

Simplified analyses in previous studies indicated that a design optimization of the insulator will be needed to achieve the no-core-melt goal. Shan [1] concluded that 2% of the rated reactor power can be removed through radiation-conduction-convection mechanisms from fuel bundles to the moderator. Although the geometric details in this reference have since been outdated, it is likely that through a design optimization similar or better results can be achieved. Licht [2] estimated that no-core-melt goal can be met if the heat transfer rate from the fuel channels is close to 3% of the rated reactor power. Licht [3] also identified knowledge gaps and further research areas to better understand insulator performance and heat transfer during accident conditions.

This paper presents a detailed analysis methodology that evaluates the heat transfer from fuel channels to the moderator. It takes into account the gaps between various fuel channel components, gap and contact heat transfer resistances, and the coupling of thermal and structural analyses.

1. Methods

1.1 Geometry

As part of the coupled thermal/stress simulation, a thin ring quadrant of 0.5[mm] axial length (seen in the figure below) was modelled using the following dimensions:

Component	Inner Radius [mm]	Outer Radius [mm]
Inner Liner	72.0	72.5
Gap One	72.5	73.0
Insulator	73.0	76.0
Gap Two	76.0	76.5
Outer Liner	76.5	77.0
Gap Three	77.0	78.5
Pressure Tube	78.5	90.5

Table 1: Reference design dimensions

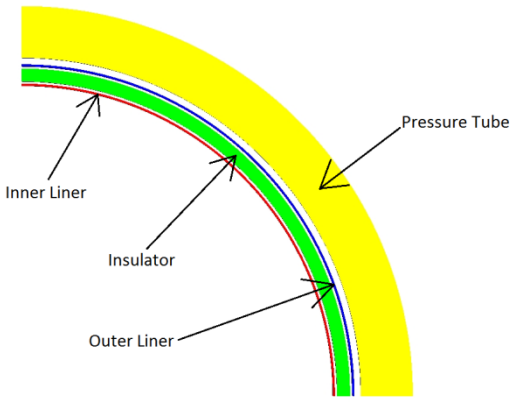

Figure 1: Thin ring quadrant used in coupled thermal/stress simulations

1.2 Mesh characteristics

The geometry described previously was meshed with sixty-four equally sized segments in the circumferential dimension. The cross-sections of these segments were maintained uniform, with dimensions of 0.5[mm] x 0.5[mm]. In addition, the water gaps were meshed with contact elements in order to circumvent the numerical ill-conditioning problems typical of volume elements as their lengths approach zero:

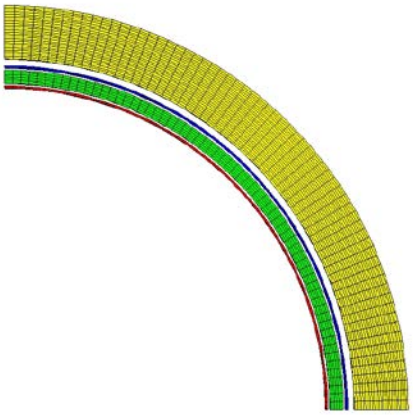

Figure 2: Axis-symmetric mesh used for fuel channel components

1.3 Fluid/material properties

1.3.1 Thermal analysis

Given the large temperature gradients expected in both normal and accident operating conditions, temperature-dependent thermal properties were used in the simulations. The relevant water/steam data were compiled from NIST [4] for pressures of 25[MPa] (normal operation) and 100[kPa] (LOCA), and a temperature range of 300[°K] to 1275[°K]. Above this upper limit, data from IAPWS-IF97 [5] were used in conjunction with non-linear curve fitting tools available in Matlab:

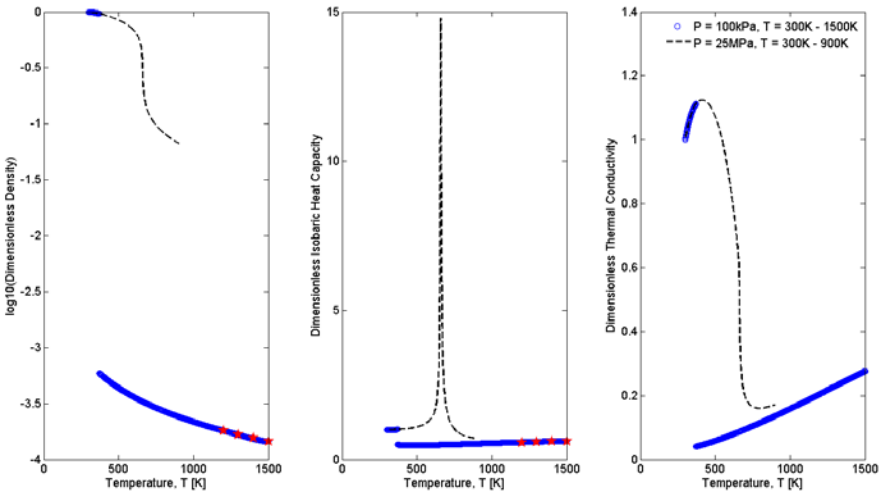

Figure 3: Dimensionless density (left), constant-pressure specific heat capacity (center), and thermal conductivity (right). All data is non-dimensionalized using the properties at T = 300[°K]. The red stars symbolize data taken from IAPWS-97 for T > 1275[°K], for which fluid properties from NIST were unavailable.

As is evident from the figure on the previous page, the polynomial curve fits for T > 1275[°K] agree well with the selected data gleaned from IAPWS. However, one important caveat should be issued regarding the thermal conductivity data. Because neither the NIST nor IAPWS websites had conductivity data available for temperatures over 1275[°K], a linear relationship was used to extrapolate beyond 1275[°K] to the required 1500[°K]. This approach would appear to be valid, as both NIST and IAPWS conductivity data in the vicinity of (but not exceeding) T = 1275[°K] are very nearly linearly related to temperature.

The data presented above were exported to VrSuite's material library in tabular format. When utilized in unison with the computed temperature distributions, the appropriate water/steam properties may be extracted from the tables at each time-step for use in calculating the contact conductance across each interface. Specifically, this is done by interpolation (between nodes) to calculate the temperature and corresponding fluid properties at the Gauss point of the contact element. In turn, this facilitates computation of an average contact conductance at the centroid of the element which is updated at each time-step.

In general, the thermal conductivities of the zirconium alloy pressure tube, Yttria-stabilized insulator, and stainless steel liners are temperature-dependent. These values, supplied by AECL[4], are as follows:

	Pressure Tube (Zirconium Alloy)	Insulator (Yttria-Stabilized Zirconia)	Liner Tubes (Stainless Steel 310)
Thermal Conductivity [W/m°K]	$27.39+\frac{9{,}687.14*T-1.26e7}{(T-1{,}067.64)^2+3.97e5}$	1.8	$0.024*T+5.0$

Table 2: Thermal conductivity as a function of temperature for the fuel channel components.

1.3.2 Stress analysis

Temperature-dependent mechanical properties were provided by AECL[4], and are summarized in the table below:

	Pressure Tube (Zirconium Alloy)	Insulator (Yttria-Stabilized Zirconia)	Liner Tubes (Stainless Steel 310)
Thermal Expansion Coeff. [1/°K]	6.58E-06	1.07E-05	$4.5e-9*T+1.35e-5$
Young's Modulus [Pa]	9.79E+11	2.00E+11	$-6.44e4*T^2+6e6*T+2e11$
Poisson's Ratio	0.33	0.33	0.33

Table 3: Mechanical properties for the fuel channel components.

[4] Verified using independent sources [6][7].

1.4 Boundary conditions

1.4.1 Thermal analysis – normal operation

For normal operation, forced convection was applied at the inner surface of the inner liner to simulate the upward flow of coolant through the fuel channel. Similarly, a natural convection boundary condition was applied at the outer surface of the pressure tube to replicate heat transferred to the moderator under buoyant action.

The ambient temperatures and pressures of the inlet, outlet, and moderator (for very thin cross-sections) are as follows [2]:

- Inlet: T_∞ = 623[°K], P = 25[MPa]
- Outlet: T_∞ = 898[°K], P=25[MPa]
- Moderator: T_∞ = 353[°K], P=300[kPa]

In conjunction with the conditions above, the Dittus-Boelter [8] equation was used to estimate the heat transfer coefficient at the inner liner, as follows:

$$\boldsymbol{h = \frac{k_c}{D_h}\left(0.023 Re^{4/5} Pr^{2/5}\right)} \quad (1)$$

Where k_c is the thermal conductivity of the coolant, D_h is the hydraulic diameter between the inner liner and center pin, Re is the Reynold's number, and Pr is the Prandtl number.

Churchill and Chu's [9] correlation for free convection on a vertical wall was utilized at the outside of the pressure tube, as is displayed below:

$$\boldsymbol{h = \frac{k_m}{L}\left[0.825 + \frac{0.387 Ra_L^{1/6}}{\left(1+(0.492/\mathrm{Pr})^{9/16}\right)^{4/9}}\right]^2} \quad (2)$$

Where k_m is the thermal conductivity of the moderator, L is the length of the fuel channel, and Ra_L is the Rayleigh number, defined as follows:

$$\boldsymbol{Ra_L = Gr_L \,\mathrm{Pr} = \frac{g\beta c_P \rho^2}{\mu k_m}(T_s - T_\infty)L^3} \quad (3)$$

Where Gr_L is the Grashof number, g is the acceleration due to gravity, β is the moderator volumetric thermal expansion coefficient (expressed in this investigation as $\beta(T_f)$ = 1.6E-5 + 9.6E-6* T_f [10], with T_f being the film temperature), c_P is the constant-pressure specific heat capacity, ρ is the moderator density, μ is the dynamic viscosity, T_s is the pressure tube surface temperature, and T_∞ is the ambient moderator temperature.

Calculation of the coolant-side heat transfer coefficient was straightforward, as the fluid properties were evaluated at the mean bulk fluid temperature (i.e. the arithmetic average of the inlet and outlet ambient coolant temperatures). This implies that the heat transfer coefficient is independent of the inner liner temperature, and thus may be considered constant.

In contrast, the moderator-side coefficient depends strongly upon the pressure tube surface temperature, both through the Rayleigh number and fluid properties, which must be evaluated at the film temperature. Since this pressure tube surface temperature is unknown *a priori*, the heat transfer coefficient must be re-calculated at each time-step using the surface temperature from the preceding time-step. In VrSuite, this may be done by expressing the coefficient as a polynomial function of the surface temperature. The polynomial was generated by fitting a curve to Churchill and Chu's correlation over a range of surface temperatures from 363[°K] to 420[°K], as is shown in the figure below:

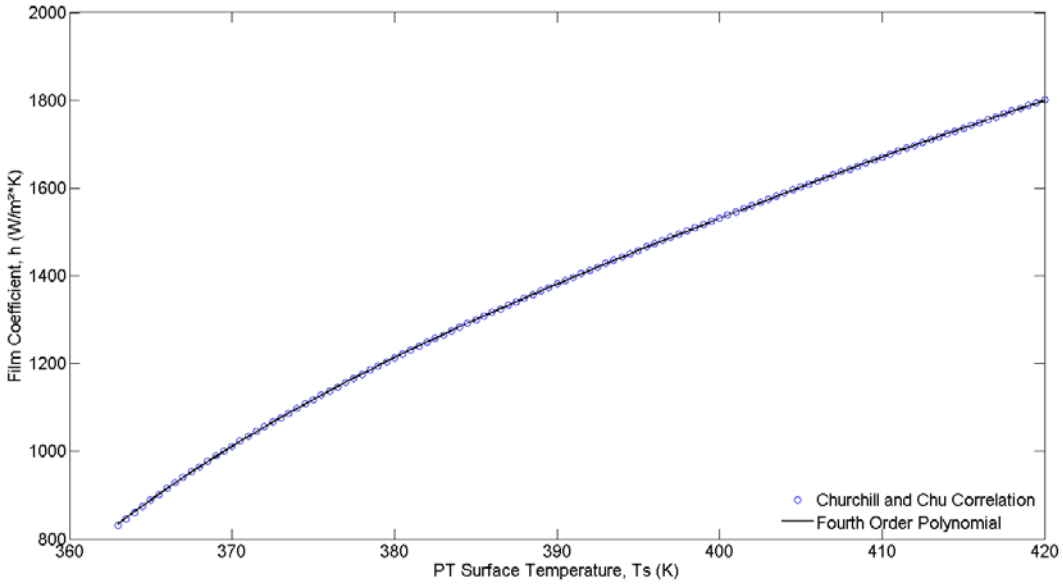

Figure 4: Heat transfer coefficient versus pressure tube surface temperature using Churchill and Chu's correlation for free convection on a vertical tube. The fitted quartic polynomial is also shown.

Worthy of note is the seemingly arbitrary selection for the lower temperature bound (i.e. T_s = 363[°K]). While a more intuitive option would be T_s = 353[°K], such that $T_s = T_\infty$ and $Ra_L = 0$, this range yielded a particularly poor goodness of fit when compared with that seen in Figure 4. Thus, the four fuel channel components were given a uniform initial temperature of 363[°K] such that subsequent heat transfer coefficients would closely conform to equation (2).

It also warrants mentioning that while it would be desirable to input equation (2) into the software in-lieu of an inexact polynomial, VrSuite does not support the fractional exponents characteristic of (2).

1.4.2 Thermal analysis – LOCA

The conditions in a Loss of Coolant Accident may be summarized as follows [2]:

- Fuel cladding: T_f = 1723[°K]
- Moderator: T_∞ = 373[°K], P = 300[kPa]

Due to the absence of coolant water characterized by a LOCA, the primary mechanism of heat transfer between the fuel bundle and inner steel liner is thermal radiation. Thus, the forced convection boundary condition used in normal operation was replaced by a radiation conductance in accident condition simulations, as shown [11]:

$$h = \sigma \epsilon F (T_f^2 + T_l^2)(T_f + T_l) \quad (4)$$

Where σ is the Stefan-Boltzmann constant, ε is the emissivity (which, for simplicity, was assumed to be independent of temperature), F is the view factor between the equivalent cylinder (see below) and inner liner, T_f is the LOCA fuel cladding temperature, and T_l is the inner liner temperature.

In order to avoid the complexity associated with the view factor between the fuel pellets and inner liner, the bundle was replaced with a single, concentric cylinder; a concept inspired by previous work with no-core-melt performed by AECL [2]. The resulting view factor for finite lengths may be expressed analytically, and is readily found in the relevant literature. However, the matter may be made even simpler yet for cylinders with lengths far exceeding their radii (i.e. $L/r \rightarrow \infty$), wherein the view factor approaches unity [12]. For the configuration described in this paper, a channel length of 10[m] and inner liner radius of 0.072[m] yields a ratio of approximately 140. Therefore, to avert the complications associated with selecting the radius of the inner cylinder, the view factor was taken to be unity in all accident scenario simulations.

When equation (4) is considered, it is clear that the radiative conductance will be subject to the same complications discussed prior with the moderator-side heat transfer coefficient. Namely, the liner temperature, T_l, is unknown *a priori* and the conductance must be calculated from the liner surface temperature computed at the previous time-step. In this case, equation (4) may be expanded to form a cubic function of liner temperature, which may be inputted into the software to calculate the conductance at each time-step.

The moderator-side heat transfer coefficient was estimated in an identical manner as that in normal operation, with only the ambient moderator temperature being changed.

1.4.3 Stress analysis

A stress simulation was performed for both normal operation and LOCA conditions, subject to the boundary conditions described in the figure on the following page:

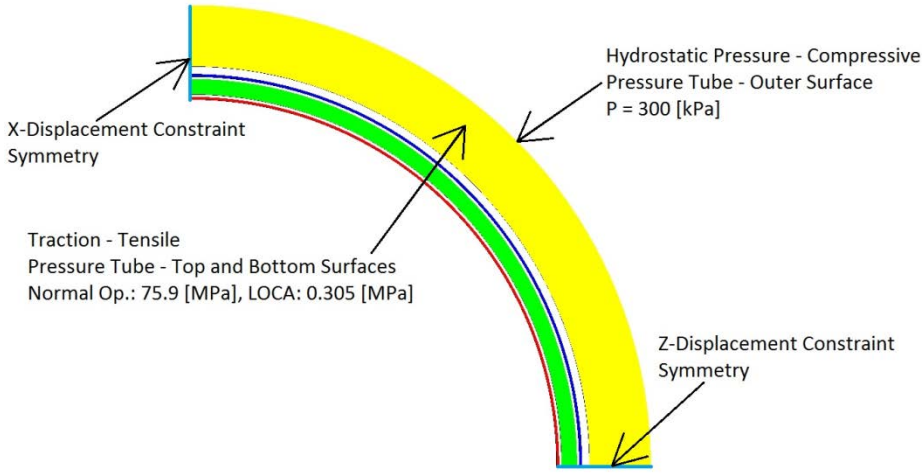

Figure 5: Boundary conditions used in the FEM stress analyses. Unless otherwise stated, a hydrostatic pressure of 25[MPa] (normal operation) or 100[kPa] (LOCA) acts on every surface.

1.5 Initial conditions

The start-up procedure for CANDU reactors entails a slow "ramping-up" of the coolant and moderator temperatures/pressures from some initial state to the normal operating conditions detailed in 2.4.1 Thermal analysis - normal operation. Since the time rate of change of coolant/moderator temperature is unavailable over the course of this process, it is difficult to accurately predict the temperature distribution through the fuel channel at intermediate times. Thus, a uniform temperature of 363[°K] was used to initialize the simulations for normal operation, the rationale for this selection being explained in section 2.4.1 Thermal analysis - normal operation. From these initial conditions, the simulations were permitted to progress to steady-state.

For the LOCA scenario analyses, the steady-state temperature distributions and component deformations under normal operation were used as an initial state.

1.6 Numerical model

1.6.1 Coupling of thermal/stress simulations

The imperativeness of thermal and stress solver coupling is best illustrated when the relationship between thermal flux and contact conductance is considered:

$$q = \Omega_i (T^+ - T^-) \quad (5)$$

Where q is the thermal flux, T^+ and T^- are the temperatures on either side of the interface, and the contact conductance, Ω_i, may be expressed as follows [11][13]:

$$\Omega_i = \Omega_{Cond} + \Omega_{Conv} + \Omega_{Rad} + \Omega_{Asp} \quad (6)$$

Since the conductances due to convection, radiation, and asperities are not currently modelled in VrSuite, conduction is the sole mechanism of heat transfer through the fuel channel. This conductance via conduction is calculated as follows:

$$\Omega_{Cond} = \frac{k}{W} \quad (7)$$

Where k is the thermal conductivity of the interface medium and W is the width of the interface. As both the conductivity and width vary with interface temperature and time, both of these variables, and thus the thermal conductance, are permitted to change under the combined thermal and mechanical loads. In order to accurately capture this complex interaction between thermal and stress effects, the respective solvers were coupled together as depicted in the following block diagram:

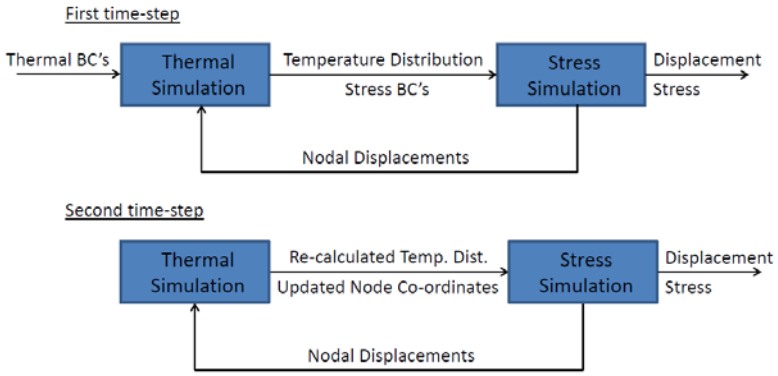

Figure 6: Block diagram depicting the data flow of a coupled thermal/stress simulation.

By exporting the displacements from the stress solver to the thermal solver at each time-step, the software is able to track the relative motion of the fuel channel components and, in turn, facilitates calculation of the changing thermal conductances.

However, it is perhaps sensible at this point to address one potential obstacle in the procedure described above. Namely, it is conceivable that when the channel components are subjected to large temperatures (and therefore, large thermal strains), two or more of them may come into close proximity. One may recall from equation (7) that thermal conductance due to conduction exhibits an inversely proportional relationship with the gap width. Thus, in the event that two components do come into close proximity, the thermal conductance may become unbounded. To circumvent this possibility, a "maximum conductance" has been implemented into VrSuite, as is explained in the figure on the next page:

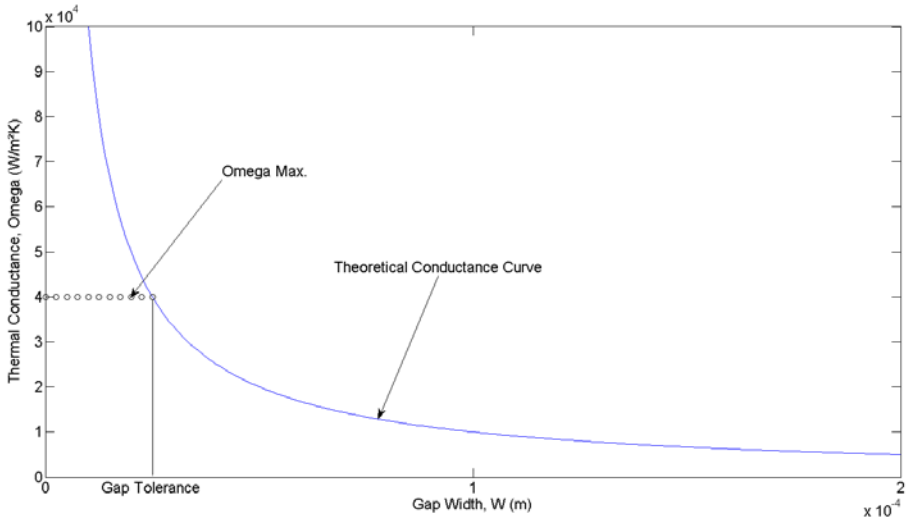

Figure 7: Demonstration of the maximum conductance concept used to avoid unboundedness for thin water interfaces. This particular example utilizes a maximum conductance of Ω_{Max} = 40,000[W/m²°K] and thermal conductivity of k = 1.0[W/m°K].

When the gap contracts to the threshold gap tolerance seen in Figure 7, the thermal conductance is re-assigned the value Ω_{Max} for all deformations with gap width less than the gap tolerance. This allows the simulation to progress without the thermal conductances and fluxes becoming unbounded.

1.6.2 Simulation parameters

VrSuite was utilized to solve the transient heat equation in cylindrical coordinates [14], as displayed below:

$$\nabla(k\nabla T) = \frac{1}{r}\frac{\partial}{\partial r}\left(kr\frac{\partial T}{\partial r}\right) + \frac{1}{r^2}\frac{\partial}{\partial \theta}\left(k\frac{\partial T}{\partial \theta}\right) + \frac{\partial}{\partial z}\left(k\frac{\partial T}{\partial z}\right) = \rho c_P \frac{\partial T}{\partial t} \quad (8)$$

Given the symmetry in the circumferential dimension and the small height of the segment being analyzed, the temperature variation in the θ and z dimensions may, in theory, be neglected. However, by default VrSuite solves equation (8) in all three dimensions.

In all coupled thermal/stress simulations described in this paper, sufficiently long durations were selected to allow the transient solution to decay to zero, leaving the steady-state temperature distribution. These selected durations, as well as the resulting global maximum temperature changes in the final time-step (i.e. $\Delta T_{Max}^{N} = |\Delta T_{Max}^{N} - \Delta T_{Max}^{N-1}|$), have been summarized in the following table:

	Normal Operation (Inlet)	Normal Operation (Outlet)	LOCA
Simulation Duration [s]	400	400	400
Global Max. Temperature Change [°K]	5.17E-05	2.74E-04	4.04E-04

Table 4: Analysis durations and temperature changes at the N^{th} time-step. All simulations use a time-step size of $\Delta t = 1.0$[s].

It is apparent from the table above that, when used in conjunction with a time-step of $\Delta t = 1.0$[s], the simulation durations selected were sufficient to ensure that the solutions had nearly ceased changing at the N^{th} time-step.

2. Results and discussion

In order to compute the thermal fluxes, the steady-state temperature distributions were plotted along a radial line through the ring quadrant:

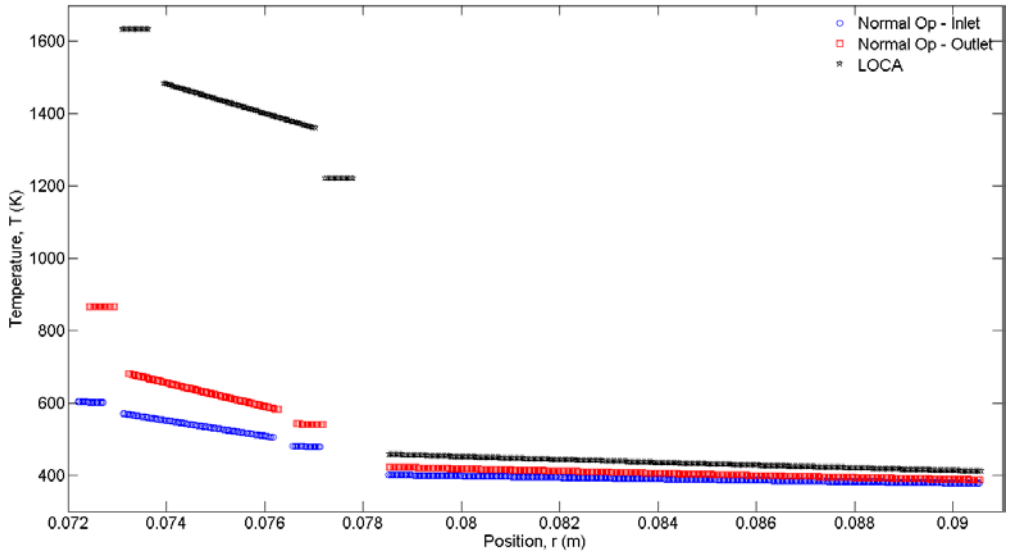

Figure 8: Steady-state temperature distribution plotted along a radial line for normal operation and accident conditions.

The steady-state thermal flux between any two points, i and j, along a radial line may be determined via the following equation:

$$q_{ij} = k_{ij,Avg} \frac{T_i - T_j}{\ln(R_j / R_i)} \quad (9)$$

Where T_i and T_j are the temperatures at points i and j, respectively, R_i and T_j are the radii at points i and j, respectively, and $k_{ij,Avg}$ is the thermal conductivity evaluated at the arithmetic average temperature of T_i and T_j. Equation (9) yields the following thermal fluxes:

- q = 2,792 [W/m] at the inlet in normal operation
- q = 4,287 [W/m] at the outlet in normal operation
- q = 5,496 [W/m] in accident conditions

It is perhaps prudent at this point to reiterate the objective of the no-core-melt feature; to minimize the heat lost by the fuel bundle to the moderator during normal operation while maximizing heat rejection in LOCA conditions. Upon first glance, it would appear that the reference fuel channel design satisfies these criteria. The thermal flux to the moderator in accident conditions is approximately 2 and 1.25 times larger than those in normal operation occurring at the inlet and outlet, respectively.

3. Future considerations

3.1 Validation

Preliminary assessments of no-core-melt in the Gen. IV Canadian SCWR have been performed by others, and their findings are readily available in the literature. Although many of these results have been rendered somewhat dated due to iterations in the reactor design, the observations made in this paper should be quantitatively compared with those results in order to validate the FEM analysis. Specifically, this will be done by adjusting the model described in this paper to be similar to those used by previous researchers [1][2][3].

3.2 Ray tracing

For accident conditions, the current model utilizes an equivalent, concentric cylinder to approximate radiative heat exchange between the 64-pin fuel bundle and inner liner. This technique allows for convenient circumvention of complicated view factors. However, ray tracing software (Siemens NX 8.5) is intended to supersede this simplification in order to more accurately simulate radiation incident upon the inner liner from the fuel bundle.

3.3 Component interference/conductance via asperities

Due to the high fuel temperatures accompanying a LOCA, the fuel channel components may be subjected to large thermal strains resulting in elastic deformations. If the magnitude of these deformations is sufficiently large, two or more of the components may come into physical contact; a highly desirable consequence as heat will transfer through the enmeshing asperities, thus increasing the rate of heat rejection to the moderator in accident conditions. The thermal conductance due to physical contact between parts may be approximated by [11][13].

$$h_{Asp} = \beta(\sigma \cdot n)^{\alpha} \quad (10)$$

Where α and β are functions of temperature and the properties of the interface, σ is the stress tensor, and n is the normal vector.

From Figure 8 it is apparent that this phenomenon is not present at steady-state. However, previous simulations (not shown in this paper for brevity) have demonstrated complex behaviour such as periodic interface contraction and expansion over the 400[s] duration. Although investigation of such transient behaviour is beyond the scope of this paper, future research may seek to study in detail the time evolution of such effects. To do so effectively, the following issues would have to be addressed within the VrSuite software:

- Support for detection of physical contact between parts, superseding unrealistic "overlapping" of components.
- Compilation of detailed data for the constants σ and β in equation (10)

3.4 Optimization of fuel channel design

Although some of the fuel channel assembly dimensions are to remain fixed (i.e. constrained by the governing nuclear physics), the remaining components/clearances may be varied in size in order to investigate the consequences upon the resulting temperature distribution. This would involve varying one or more of the parameters at a time between a pre-determined minimum and maximum value, with designs between these bounds prescribed by global optimization. The merit of each design would be evaluated for a given objective function calculated at each sampling point in the design space. In this way, the optimum combination of parameters could be found in the design space. This procedure should allow for a fuel channel design which attains a state of no-core-melt in the most efficient manner possible.

4. Conclusion

The purpose of this paper was to develop a numerical model for the assessment of the no-core-melt argument in the Generation IV Canadian SCWR. By simulating the conditions predicted at both normal operation and at LOCA, the thermal flux and structural deformations were calculated for the reference design fuel channel. These calculations suggested that, with appropriate selections of component sizes, materials, and gaps between components, a state of no-core-melt may be attainable in the event of LOCA with no emergency core cooling.

This report also identified several areas warranting further consideration in the future. Chief among those is the optimization of the fuel channel design, wherein the dimensions will be varied in order to ascertain the configuration which best achieves no-core-melt.

5. Acknowledgements

The authors would like to thank Natural Resources Canada (NRCan) and the National Sciences and Engineering Research Council (NSERC) for their support of the Canadian Generation IV National Program.

6. Bibliography

[1] Shan, J; Jiang, Y; Leung, L.K.H. (March 2011). “Subchannel and Radiation Heat Transfer Analysis of 54-Element CANDU-SCWR Bundle”, The 5th International Symposium on Supercritical Water-Cooled Reactors (ISSCWR-5), Vancouver, British Columbia, Canada, March 13-16, 2011.

[2] Licht, J; Xu, R. (April 2012). "Preliminary No-Core-Melt Assessment for the High Efficiency Channel Preconceptual Design", The 3rd China-Canada Joint Workshop on Supercritical-Water-Cooled Reactors, Xi'an, China, April 18-20, 2012.

[3] Licht, J. (March 2013). "Moderator Cooling Requirements for the Canadian SCWR", The 6th International Symposium on Supercritical Water-Cooled Reactors (ISSCWR-6), Shenzhen, Guangdong, China, March 03-07, 2013.

[4] National Institute of Standards and Technology. Thermophysical Properties of Fluid Systems. Retrieved from http://webbook.nist.gove/chemistry/fluid/

[5] The International Association for the Properties of Water and Steam. Zittau's Fluid Property Calculator. Retrieved from http://thermodynamik.hs-zigr.de/fpc/index.php

[6] International Atomic Energy Agency. (June 2006). "Thermophysical properties database of materials for light water reactors and heavy water reactors", Final report of a coordinated research project (1999-2005).

[7] Schlichting, K.W., Padture, N.P., Klemens, P.G. "Thermal conductivity of dense and porous yttria-stabilized zirconia", *Journal of Materials Science* 36 (2001) 3003-3010.

[8] Winterton, R.H.S. Where did the Dittus and Boelter equation come from? Retrieved from http://herve.lemonnier.sci.free.fr/TPF/NE/Winterton.pdf

[9] Incropera, Frank P; DeWitt, D (2000). Fundamentals of Heat and Mass Transfer (4th Ed.). Hoboken, NJ. John Wiley and Sons, Inc.

[10] H_2O Thermal Expansion Coefficient. Retrieved from http://physchem.kfunigraz.ac.at/sm/Service/Water/H2Othermexp.htm

[11] Goldak, J; Aldea, V; Zhou, J; Wang, S; Mocanita, M; Downey, D; Wang, B. (November 18, 2000). "Coupled Thermal Stress Analysis in Die Casting: A Contact Problem", First M.I.T. Conference on Computational Fluid and Solid Mechanics, Cambridge, Massachusetts, USA, June 12-14, 2001.

[12] Howell, J. R.; Siegel, R; Menguç, M. P. (2011). Thermal Radiation Heat Transfer (5th Ed.). Boca Raton, FL. CRC Press, Taylor and Francis Group.

[13] Song, S; Yovanovich, M. M.; Goodman, F. O. (August 1993). "Thermal Gap Conductance of Conforming Surfaces in Contact".

[14] Çengel, Y. A. (2007). Heat and Mass Transfer - A Practical Approach (3rd Ed.). McGraw-Hill Education.